Preliminary results towards the mechanical characterization of cellulose nanofibers using HarmoniX mode atomic force microscopy

Cite as: AIP Conference Proceedings **2416**, 020011 (2021); https://doi.org/10.1063/5.0068542
Published Online: 05 November 2021

Taljinder Singh, Pierfrancesco Atanasio, Daniele Schiavi, et al.

Preliminary Results Towards the Mechanical Characterization of Cellulose Nanofibers Using HarmoniX Mode Atomic Force Microscopy

Taljinder Singh[1], Pierfrancesco Atanasio[1], Daniele Schiavi[2], Veronica Di Lorenzo[2], Francesca Anna Scaramuzzo[1], Daniele Passeri[1,3,a)], Giorgio Mariano Balestra[2] and Marco Rossi[1,3]

[1]*Department of Basic and Applied Sciences for Engineering, Sapienza University of Rome, Via A. Scarpa 14, 00161 Rome, Italy.*

[2]*Department of Agricultural and Forest Sciences (DAFNE), University of Tuscia, Via S. Camillo De Lellis snc, 01100 Viterbo (Italy)*

[3]*Research Center for Nanotechnology applied to Engineering of Sapienza University of Rome (CNIS), Piazzale A. Moro 5, 00185 Rome, Italy*

[a)]Corresponding author: daniele.passeri@uniroma1.it

Abstract. The characterization of mechanical properties of cellulose based nanomaterials at the nanometer scale is fundamental in the development and optimization of a broad range of technological products where these nanomaterials are used for their unique physical and chemical properties. HarmoniX is an atomic force microscopy (AFM) based technique which takes advantage of the use of a T-shaped cantilever, the torsion of which is excited during the surface scan in tapping mode. This results in a torsional signal that can be analyzed in real time to map, simultaneously to the topographic reconstruction, sample mechanical properties like the elastic modulus, tip-sample adhesion, or energy dissipation during the indentation cycle. Here we report preliminary results concerning the capability of HarmoniX to characterize the mechanical properties of nanocellulose fibers from hazelnut tree shells previously separated from their matrix via chemical treatment.

INTRODUCTION

Cellulose and nanocellulose can be a valid solution to various environmental problems, representing an ecosustainable alternative that can potentially replace polluting and non-recyclable materials in many uses. Cellulose is the most abundant organic compound on Earth and it is the main constituent of plant fiber, it is used in various fields around the world due to its availability, biocompatibility, biological degradability and sustainability. Similarly, nanocellulose extracted from agricultural waste, is gaining attention for its exceptional mechanical and thermal properties, as well as for environmental compatibility and affordability. The use of a by-product of important agricultural residues or food crops for fibrous applications will benefit the environment by saving the natural resources required to produce natural and synthetic fibers. The term nanocellulose (NC) refers to cellulosic extracts or treated materials having structural dimensions at the nanometer scale. Cellulose can be extracted from various natural sources such as wood pulp, sunflower, pinecones, fruit and vegetable pomace, sago seed shells, sugar cane bagasse, rice husk, bacteria, waste products in wood processing and from agricultural wastes [1]. Since it originates from renewable matter, or can even be obtained by low-value wastes, and thanks to its abundance in nature, cellulose represents an intrinsically safe and 'green' resource, which could revolutionize the sciences of materials and biomaterials. Extraction of cellulose from lignocellulosic sources may be conducted by several and sometimes sequential mechanical and chemical methods. In order to obtain NC, cellulose must undergo controlled acidic hydrolysis (usually with sulfuric acid), or enzymatic hydrolysis. There are three main classes of NC: cellulose nanocrystals (CNCs), cellulose nanofibers (CNFs) and bacterial nanocellulose (BNC). These families differ from each other for their source, functions, applications and size

NanoInnovation 2020
AIP Conf. Proc. 2416, 020011-1–020011-7; https://doi.org/10.1063/5.0068542
Published by AIP Publishing. 978-0-7354-4133-0/$30.00

of the isolated cellulosic material: for example, CNCs are 5 − 10 nm wide and 100 − 300 nm long, while CNFs are 5 − 50 nm in width and up to several micrometers in length [2, 3]. However, they share unique properties such as high aspect ratio, low density, biodegradability, great strength and rigidity. Due to their mechanical and chemical properties (i.e. flexibility, resistance, high aspect ratio), CNFs found applications in different fields and are extremely promising as a component of innovative industrial products. It is extremely suitable as a reinforcement in composite materials such as high density polyethylene (HDPE) [4] or to build composite materials to replace plastics [5], such an application can cover many different fields like food packaging [6, 7] thanks to the oxygen barrier properties due to their density and highly crystallinity [8]. However, CNFs have also been studied for medical applications such as pharmaceuticals, biomedical and drug delivery [9, 10], environmental applications such as water purification [11] and recycled paper production [12], but also in the electrochemical field as a thin film electrodes for supercapacitors [13]. Therefore, due to the wide range of applications the capability to characterize the mechanical properties of CNFs at the nanometer scale is extremely important from both a scientific and technological point of view. Really, given their characteristic dimensions, methods are required which can determine the mechanical properties of NC samples by positioning the measuring probe on selected locations of the sample with nanometer lateral resolution and testing a nanometer-sized volume of the sample. These requirements suggested the use of nanomechanical methods based on atomic force microscopy (AFM), where a nanometer sized probe is used to reconstruct the morphology of the sample, can be positioned at selected locations of the surface, can test the mechanical response of the material, and can map the determined mechanical parameters on the sample surface simultaneously to the morphological reconstruction [14]. Among the different AFM based techniques for the mechanical characterization at the nanometer scale, HarmoniX mode is a method where a T-shaped cantilever is used to reconstruct the sample morphology in tapping mode [15]. During the tapping, the out-of-axis tip periodically indents the sample surface resulting in the excitation of torsional oscillations of the cantilever. The cantilever torsional signal is acquired an analyzed to extract force-distance curves. These latter allow the mapping in real time of different mechanical parameters including the sample indentation modulus, the tip-sample adhesion force, and the energy dissipated during the tapping due to the tip-sample contact [16, 17]. HarmoniX can be successfully used to mechanically characterize soft materials in a relatively broad range of elastic modulus, i.e., from about 1 MPa to 10 GPa [18]. HarmoniX has been used to study polymers, polymer blends, and polymers reinforced with nanomaterials [19–22], bacterial nanowires [23], nanoparticles internalized in cells [24], resin-embedded wheat aleurone particles [25].

In this work, the results of a preliminary study aimed at exploring the capability of HarmoniX to characterize the mechanical properties of NC fibers obtained from hazelnut tree shells have been reported. First, NC fibers have been imaged using scanning electron microscopy (SEM). Quantitative morphological investigation of the obtained nanomaterial was performed through AFM. Finally, accurate quantitative mapping of mechanical modulus has been carried out in order to assess the effectiveness of HarmoniX in the analysis of NC samples.

EXPERIMENTAL

Sample Preparation

Samples for SEM and AFM measurements were obtained by diluting NC suspension with distilled water. A dilution ratio of 1:120 and 1:1200 was used for the preparation of SEM and AFM specimens, respectively, where different dilution ratios were required to optimize the two different characterization methodologies. Drops of diluted samples were deposited on Si substrates and maintained at room temperature until complete drying.

Scanning Electron Microscopy

The surface morphology of the sample was analyzed through scanning electron microscopy (SEM). The instrument used for SEM analysis is a field emission SEM (FESEM, AURIGA, Zeiss) which was used to visualize the characteristic dimensions of the sample without any conductive coating. The acceleration voltage was set at 10 kV.

Atomic Force Microscopy

The morphology of the samples was studied using a standard AFM setup (Dimension ICON, Bruker Inc.) in tapping mode with standard Si cantilevers (RTESP, Bruker Inc.), in air and at room conditions.

Mechanical characterization of the samples was performed in HarmoniX mode using the same AFM instrumentation

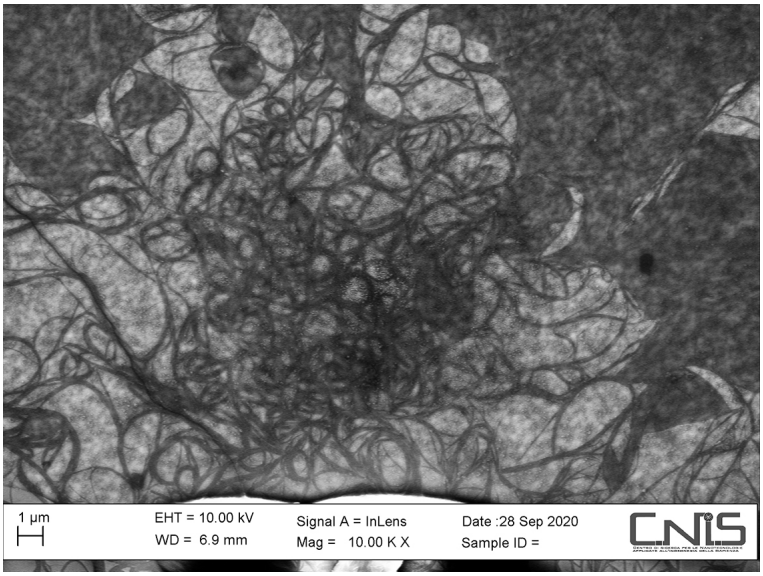

FIGURE 1. SEM image of the sample surface showing bundles of cellulose fibers.

equipped with HMX-10 (Bruker Inc.) probes, in air and at room conditions. Quantitative maps of indentation modulus, which require the evaluation of the actual tip-sample contact radius, were obtained after calibration using a reference material constituted of a blend of polystyrene (PS), with indentation modulus of 2 GPa, and low density polyethylene (LDPE), with indentation modulus of 100 MPa (PS-LDPE sample, Bruker Inc.).

RESULTS AND DISCUSSION

Figure 1 shows a typical SEM image of the surface of the sample showing the presence of bundles of cellulose fibers with sub-micrometer diameter and length from tens to hundreds of microns. The structure of the observed fibers was analyzed using AFM. Figure 2 shows typical AFM data for the fibers at two different magnifications, including the topography reporting the quantitative value of the local height of the sample (Fig. 2a and d), the amplitude error image which enable one to visualize the fine details of the surface (Fig. 2b and e), and the phase image (Fig. 2c and f) which reflects the not homogeneous energy dissipation at the tip-sample contact during each tapping cycle [26], thus enabling one to clearly distinguish the fibers from the substrate. AFM characterization clearly indicates that the fibers are actually composed of bundles of CNFs with diameter of $50 - 60$ nm and micrometric length. Therefore, SEM and AFM morphological characterizations indicate that cellulose nanofibers were actually isolated from hazelnut tree shells, thus confirming the effectiveness of the applied protocols for the treatment of lignocellulosic residues from the agrifood supply chain.

In order to verify its capability to map the transverse (i.e., along the radial direction) elastic properties of single CNFs, to serve as a preliminary study for its use in a comprehensive study on different cellulose based nanomaterials, we performed the nanomechanical characterization of the same CNFs sample using HarmoniX mode, an example of which is reported in Fig. 3. Figure 3 shows the topography of a region of sample where bundles of CNFs are visible (Fig. 3a), the corresponding images of amplitude error (Fig. 3b) and phase shift (Fig. 3c), which are analogous to those we obtained using standard AFM tapping mode. In addition, Fig. 3d shows the corresponding map of tip-sample adhesion force, which is coherent with the (qualitative) information deducible from phase image. Figure 3e shows the corresponding map of the elastic modulus after calibration using the PS-LDPE reference sample. The map indicates that the fiber is stiffer than the substrate. Indeed, after statistics on a selected area like the one indicated in Fig. 3e, the elastic modulus of the fiber can be evaluated as high as 4.1 ± 0.1 GPa, while the modulus of the substrate is evaluated as high as 2.9 ± 0.1 GPa. The values obtained for the fibers and the substrate fall within the range of applicability of HarmoniX. In particular, the value of elastic modulus of 4.1 ± 0.1 GPa obtained for the cellulose fibers seems coherent with data reported in literature. For instance, values in the range of $12 - 23$ GPa have been found using AFM

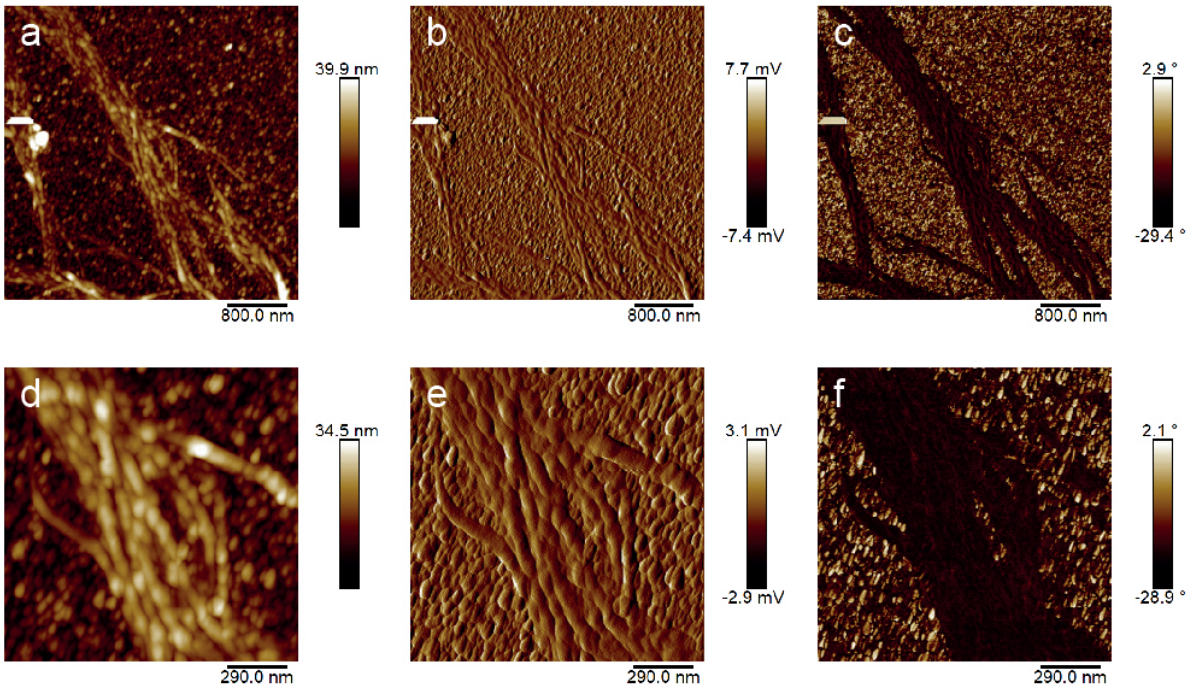

FIGURE 2. Example of AFM characterization of CNFs sample at different magnifications: topography (a and d), amplitude error (b and e), and phase images (c and f).

nanoindentations [27] while the indentation of cellulose in the wet state resulted in values of modulus in the range of tens of kilopascals [28]. Really, axial modulus values of CNFs as high as 90 − 110 GPa determined using three-point bending tests with AFM have been recently reported, which are compatible with values retrieved with X-ray diffraction on crystalline regions of fibers [29]. Conversely, elastic modulus values of 6−7 GPa have been obtained on CNFs films using tensile tests [30, 31] or three-point bending tests [32]. While the axial modulus of the fibers is often reported, the characterization of the transverse elastic modulus using AFM-based nanoindentation is rather new, and recently a value of 6.9 ± 0.4 GPa has been reported, in good agreement with our results [33]. Really, it must be noted that depending on the mechanical and geometrical parameters of the CNFs, the use of simple contact mechanics models like Hertz or Derjaguin-Muller-Toporov [34] neglecting the finite lateral dimensions of the sample may result in the incorrect evaluation of experimental data. For instance, using PeakForce Quantitative Nanomechanical Mapping (PF-QNM), an apparent modulus of isolated CNCs of 5 GPa was obtained which was eventually corrected as 20 GPa after analyzing the experimental data using finite element analysis (FEA), thus obtaining an average transverse modulus of CNCs of 8 GPa, with however a 95% confidence interval of 2.7 − 20.0 GPa considering all the possible sources of experimental uncertainty [35].

Conversely, the value of 2.9 ± 0.1 GPa obtained in correspondence of the substrate is far lower that the indentation modulus of monocrystalline Si, which can be calculated as high as 165 GPa and 175 GPa for (100) and (111) Si, respectively [36]. Actually, the expected values for Si are well above the value of about 10 GPa corresponding to the maximum of the range in which the accuracy of HarmoniX has been demonstrated [18] and, thus, the saturation of the elastic modulus channel would be expected in correspondence of the substrate. The value of 2.9 ± 0.1 GPa suggests the presence of a uniform layer of soft material on the substrate which could result from residuals of the preparation. In order to confirm this hypothesis, we performed an experiment analogous to those used in the so-called 'hole-digging method' for the measurement of the thickness of thin polymeric films on stiff substrates [37]. After imaging the same surface in tapping mode using a standard tapping mode cantilever, a square area with side of 500 nm was selected and imaged by switching the operation modality from tapping to contact mode in order to intentionally remove the layer of soft material. Figure 4 shows the result of this experiment. Figure 4a is a SEM image of the surface where the scratched area is visible. The AFM system was then switched again in tapping mode to acquire the morphology of the area. Figure 4b shows the AFM amplitude error image, which clearly indicates that the mechanical scratch

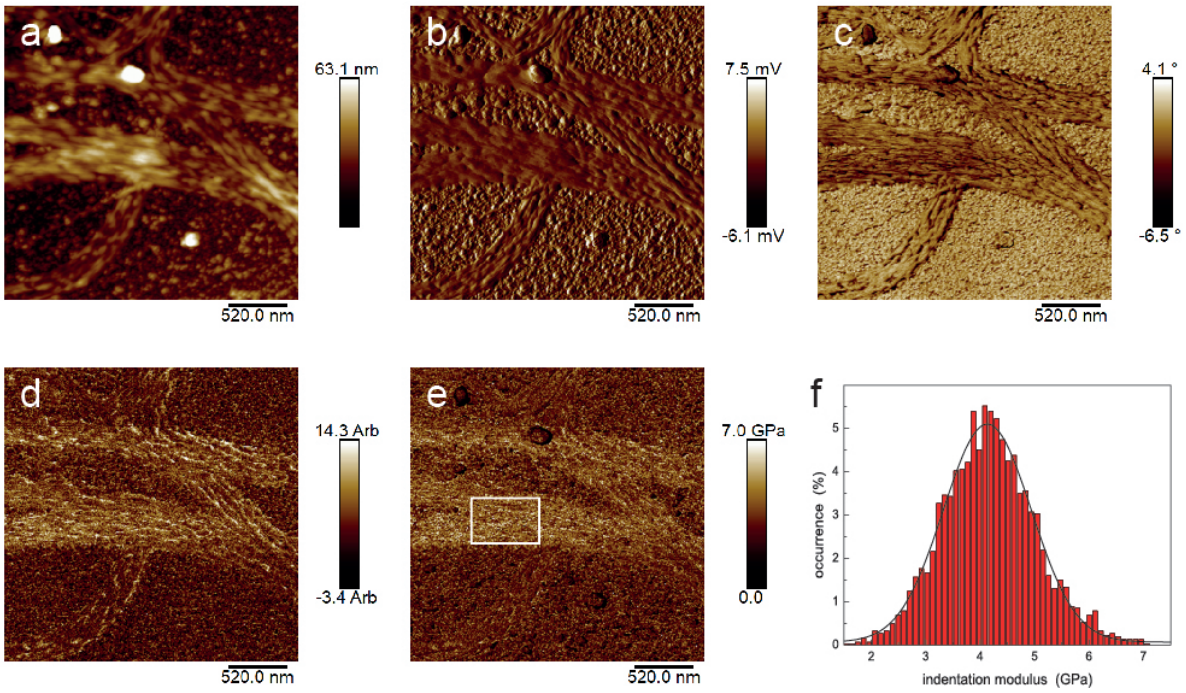

FIGURE 3. Example of nanomechanical characterization of CNFs sample using HarmoniX: (a) topography, (b) amplitude error, (c) phase, (d) adhesion force, (e) elastic modulus map, (f) statistics of the elastic modulus of the fiber calculated from the area indicated in the rectangle in (e).

removed the soft and rough layer leaving visible the stiff and flat substrate in agreement with SEM images. From the topographical image (Fig. 4c), a profile was selected (Fig. 4d) from which the thickness of the soft layer was evaluated as about 20 nm. Actually, the small value of the thickness of the layer could be responsible for the increase of the measured elastic modulus, although HarmoniX is a technique characterized by a shallow penetration into the sample [38, 39]. Really, the actual value of the elastic modulus of the layer is not interesting in itself. Nevertheless, the presence of such a layer on the nanofibers would result in an increased value of the measured diameter of the fibers. Also, as the layer is softer than the CNFs, its presence would result in a reduction of the apparent elastic modulus of the fiber. The extraction of the map of the elastic modulus of sole CNFs would require its deconvolution from the measured map of the apparent elastic modulus [40]. Really, the contrast in AFM phase images of the fibers (e.g., Fig. 2c and f or Fig. 3c) seems to suggest that the material observed on the substrate is not present on the fibers. However, while it is actually possible to isolate the nanocellulose, the treatments to which the sample was initially subjected is demonstrated to leave a high quantity of organic residuals. It is therefore advisable to consider improving the chemical treatments to have greater purity and quality of the material in order to develop innovative biobased products in the future.

CONCLUSIONS

In conclusion, a preliminary study was carried out in order to explore the capability of HarmoniX, an AFM based technique which allows the mechanical analysis of materials at the nanometer scale, to characterize cellulose nanofibers isolated from hazelnut tree shells by acid hydrolysis. SEM and AFM morphological analysis confirmed the effectiveness of the chemical treatment to obtain micrometer size bundles of CNFs with diameter of a few tens of nanometers. Nanomechanical characterization using HarmoniX allowed us to evaluate the elastic modulus of the fibers as high as 4.1 GPa, demonstrating the effectiveness of this technique for the characterization of this kind of nanomaterials. Also, the nanomechanical analysis allowed us to identify the presence of residuals of the chemical treatment which should be avoided in the future optimization of sample treatment to obtain CNFs. The great potential of cellulose based nanomaterials obtained from several plant wastes offers requires an appropriate characterization for their use as

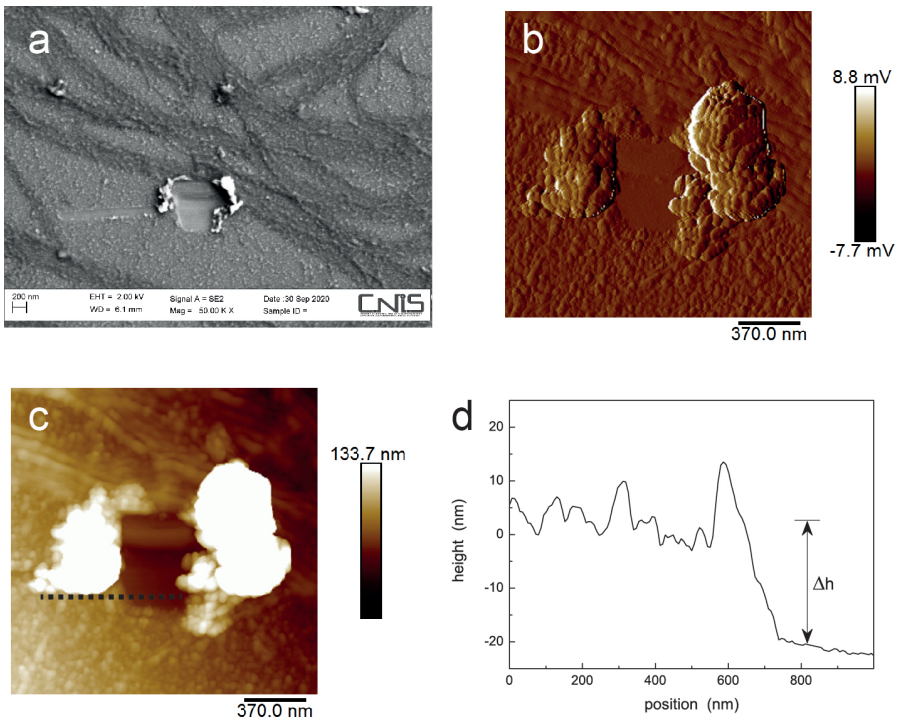

FIGURE 4. Measurement of the thickness of the layer using the hole-digging method: SEM (a), AFM amplitude error (b), and AFM morphology (c) of the scratched area and (d) profile of the dotted line indicated in (c) used to evaluate the film thickness.

green carriers of organic active ingredients useful in eco-sustainable plant protection strategies [41, 42]. The ultimate goal that we hope to achieve is to introduce nanocellulose-based solutions on the market not only as a reinforcement but also for other innovative applications. Given its characteristics as an eco-sustainable, biodegradable and renewable material, it assures greater safety for the environment and human health, representing a promising solution as sustainable product.

REFERENCES

[1] M. Sánchez-Gutiérrez, E. Espinosa, I. Bascón-Villegas, F. Pérez-Rodríguez, E. Carrasco, and A. Rodríguez, Agronomy **10**, p. 696 (2020).
[2] J. Han, C. Zhou, Y. Wu, F. Liu, and Q. Wu, Biomacromolecules **14**, 1529–1540 (2013).
[3] S. Beck-Candanedo, M. Roman, and D. G. Gray, Biomacromolecules **6**, 1048–1054 (2005).
[4] H. Yano, H. Omure, Y. Honma, H. Okumura, H. Sano, and F. Nakatsubo, Cellulose **25**, 3351–3362 (2018).
[5] A. Bhatnagar and M. Sain, J. Reinf. Plast. Comp. **24**, 1259–1268 (2005).
[6] M. Ghaderi, M. Mousavi, H. Yousefi, and M. Labbafi, Carbohyd. Polym. **104**, 59–65 (2014).
[7] M. Rossi, D. Passeri, A. Sinibaldi, M. Angjellari, E. Tamburri, A. Sorbo, E. Carata, and L. Dini, Adv. Food Nutr. Res. **82**, 149–204 (2017).
[8] J.-K. Kim, B. Choi, and J. Jin, Carbohyd. Polym. **249**, p. 116823 (2020).
[9] A. Pandey, Environ. Chem. Lett. **19**, 2043–2055 (2021).
[10] Z. Aytac, H. S. Sen, E. Durgun, and T. Uyar, Colloid. Surface. B **128**, 331–338 (2015).
[11] H. Ma, C. Burger, B. S. Hsiao, and B. Chu, J. Mater. Chem. **21**, 7507–7510 (2011).
[12] A. Balea, J. L. Sanchez-Salvador, M. C. Monte, N. Merayo, C. Negro, and A. Blanco, Molecules **24**, p. 1800 (2019).
[13] X. Wang, K. Gao, Z. Shao, X. Peng, X. Wu, and F. Wang, J. Power Sources **249**, 148–155 (2014).
[14] D. Passeri, M. Rossi, E. Tamburri, and M. L. Terranova, Anal. Bioanal. Chem. **405**, 1463–1478 (2013).
[15] O. Sahin, S. Magonov, C. Su, C. F. Quate, and O. Solgaard, Nat. Nanotechnol. **2**, 507–514 (2007).

[16] O. Sahin, C. F. Quate, O. Solgaard, and F. J. Giessibl, in *Handbook of nanotechnology*, edited by B. Bhushan (Springer, 2010), pp. 711–729.
[17] A. Sikora and Ł. Bednarz, in *Acoustic scanning probe microscopy*, edited by F. Marinello, D. Passeri, and E. Savio (Springer Berlin Heidelberg, 2013) Chap. 11,, pp. 325–3500.
[18] O. Sahin and N. Erina, Nanotechnology **19**, p. 445717 (2008).
[19] P. Schön, K. Bagdi, K. Molnár, P. Markus, B. Pukánszky, and G. J. Vancso, Eur. Polym. J. **47**, 692–698 (2011).
[20] P. Schön, S. Dutta, M. Shirazi, J. Noordermeer, and G. J. Vancso, J. Mater. Sci. **46**, 3507–3516 (2011).
[21] M. E. Dokukin and I. Sokolov, Langmuir **28**, 16060–16071 (2012).
[22] D. Passeri, A. Biagioni, M. Rossi, E. Tamburri, and M. L. Terranova, Eur. Polym. J. **49**, 991–998 (2013).
[23] K. M. Leung, G. Wanger, Q. Guo, Y. Gorby, G. Southam, W. M. Laue, and J. Yang, Soft Matter **7**, 6617–6621 (2011).
[24] M. Reggente, D. Passeri, L. Angeloni, F. A. Scaramuzzo, M. Barteri, F. De Angelis, I. Persiconi, M. E. De Stefano, and M. Rossi, Nanoscale **9**, 5671–5676 (2017).
[25] A. Berquand, C. Gaillard, and B. Bouchet, AN122, Bruker Corporation (2009).
[26] J. Tamayo and R. García, Appl. Phys. Lett. **71**, 2394–2396 (1997).
[27] N. Yildirim and S. H. Shaler, MRS Advances **1**, 639–644 (2016).
[28] J. Hellwig, V. L. Durán, and T. Pettersson, Anal. Methods **10**, 3820–3823 (2018).
[29] L. Zhai, H. C. Kim, J. W. Kim, J. Kang, and J. Kim, Cellulose **25**, 4261–4268 (2018).
[30] A. Yamakawa, S. Suzuki, T. Oku, K. Enomoto, M. Ikeda, J. Rodrigue, K. Tateiwa, Y. Terada, H. Yano, and S. Kitamura, Carbohyd. Polym. **171**, 129–135 (2017).
[31] A. Isogai, T. Saito, and H. Fukuzumi, Nanoscale **3**, 71–85 (2011).
[32] S. Sun, J. R. Mitchell, W. MacNaughtan, T. J. Foster, V. Harabagiu, Y. Song, and Q. Zheng, Biomacromolecules **11**, 126–132 (2010).
[33] M. S. Parvej, X. Wang, and L. Jiang, J. Compos. Mater. **54**, 4487–4493 (2020).
[34] B. V. Derjaguin, V. M. Muller, and Y. P. Toporov, J. Colloid Interf. Sci. **53**, 314–326 (1975).
[35] R. Wagner, R. Moon, J. Pratt, G. Shaw, and A. Raman, Nanotechnology **22**, p. 455703 (2011).
[36] D. Passeri, M. Rossi, and J. J. Vlassak, Ultramicroscopy **128**, 32–41 (2013).
[37] X. Hong, Y. Gan, and Y. Wang, Surf. Interface Anal. **43**, 1299–1303 (2011).
[38] D. Passeri, E. Tamburri, M. L. Terranova, and M. Rossi, Nanoscale **7**, 14358–14367 (2015).
[39] M. Reggente, M. Natali, D. Passeri, M. Lucci, I. Davoli, G. Pourroy, P. Masson, H. Palkowski, U. Hangen, A. Carradò, and M. Rossi, Colloid. Surface. A **532**, 244–251 (2017).
[40] D. Passeri, M. Rossi, A. Alippi, A. Bettucci, D. Manno, A. Serra, E. Filippo, M. Lucci, and I. Davoli, Superlattices Microstruct. **44**, 641–649 (2008).
[41] E. Fortunati, N. Rescignano, E. Botticella, D. La Fiandra, M. Renzi, A. Mazzaglia, L. Torre, J. M. Kenny, and G. M. Balestra, J. Plant Dis. Prot. **123**, 301–310 (2016).
[42] E. Fortunati and G. M. Balestra, in *Biomass, Biopolymer-Based Materials, and Bioenergy*, Woodhead Publishing Series in Composites Science and Engineering, edited by D. Verma, E. Fortunati, S. Jain, and X. Zhang (Woodhead Publishing, 2019), pp. 161–178.